MOLECULAR CARCINOGENESIS 49:672–683 (2010)

3,3′-Diindolylmethane Suppresses 12-*O*-Tetradecanoylphorbol-13-Acetate-Induced Inflammation and Tumor Promotion in Mouse Skin via the Downregulation of Inflammatory Mediators

Eun Ji Kim,[1] Heesook Park,[2] Jongdai Kim,[3] and Jung Han Yoon Park[1,2]*

[1]*Center for Efficacy Assessment and Development of Functional Foods and Drugs, Hallym University, Chuncheon, Korea*
[2]*Department of Food Science and Nutrition, Hallym University, Chuncheon, Korea*
[3]*Department of Food Science and Biotechnology, Kangwon National University, Chuncheon, Korea*

3,3′-Diindolylmethane (DIM) is a major acid-condensation product of indole-3-carbinol and is present in cruciferous vegetables. In this study, we evaluated the effects of DIM on antiinflammatory and antitumor promotion activity in mouse skin and explored the relevant mechanisms. When 12-*O*-tetradecanoylphorbol-13-acetate (TPA) was applied topically to the mouse ear to induce inflammation, DIM pretreatment effectively inhibited TPA-induced ear edema formation. To evaluate the mechanisms underlying DIM's antiinflammatory effects, DIM was topically treated to the shaved backs of mice 30 min before TPA treatment. DIM inhibited the TPA-induced increases in the expression of cyclooxygenase (COX)-2, inducible nitric oxide synthase (iNOS), chemokine (C-X-C motif) ligand (CXCL) 5, and interleukin (IL)-6 in mouse skin. DIM also inhibited nuclear factor-kappa B (NF-κB)'s DNA binding activity, the nuclear translocation of p65, and the degradation of inhibitor of κB (IκB) α in TPA-stimulated mouse skin. Furthermore, DIM reduced TPA-induced increases in the activity of extracellular signal regulated protein kinase (ERK)-1/2 and IκB kinase (IKK). When mouse skin papillomas were initiated via the topical application of 7,12-dimethylbenz[α]anthracene (DMBA) and promoted with repeated topical applications of TPA, repeated topical applications of DIM prior to each TPA treatment significantly suppressed the incidence and multiplicity of the papillomas. DIM also reduced the expression of COX-2 and iNOS, ERK phosphorylation, and the nuclear translocation of p65 in papillomas. Collectively, these results show that DIM exerts antiinflammatory and chemopreventive effects in mouse skin via the downregulation of COX-2, iNOS, CXCL5, and IL-6 expression, which may be mediated by reductions in NF-κB activation.

Key words: skin papilloma; inflammation; NF-κB; inducible nitric oxide synthase; cyclooxygenase

INTRODUCTION

Cancer is a significant global health problem and continues to be a leading cause of death, despite the significant advances made thus far in modern medicine. As the currently available treatment options are not wholly effective at advanced stages of malignancy, it is important to control cancer in its early stages, before malignancy manifests [1]. In this regard, chemoprevention—in which carcinogenesis is inhibited, retarded, or reversed at a premalignant stage by the use of relatively nontoxic bioactive substances—has been recognized as a promising strategy for reducing human cancer risk [2]. Therefore, it is important to find effective chemopreventive agents for successful cancer management.

Inflammation is one of the protective strategies used by hosts to remove harmful stimuli including irritants, damaged tissues, or pathogens. However, unchecked inflammation has been implicated in the development and promotion of a variety of human cancers—including breast, colon, skin, stomach, and prostate cancers [3–5]. Macrophages, the most important proinflammatory cells, generate reactive oxygen species, cytokines, growth factors, angiogenic factors, and proteases, and can thereby promote both the development of cancers and their

Abbreviations: NF-κB, nuclear factor-kappa B; IκB, inhibitor of κB; IKK, IκB kinase; COX, cyclooxygenase; iNOS, inducible nitric oxide synthase; DIM, 3,3′-diindolylmethane; LPS, lipopolysaccharide; DSS, dextran sodium sulfate; AOM, azoxymethane; TPA, 12-*O*-tetradecanoylphorbol-13-acetate; DMBA, 7,12-dimethylbenz[α]anthracene; ERK, extracellular signal-regulated kinase; MAPK, mitogen-activated protein kinase; PMSF, phenylmethylsulfonyl fluoride; DTT, dithiothreitol; PCR, polymerase chain reaction; CXCL, chemokine (C-X-C motif) ligand; IL, interleukin.

*Correspondence to: Department of Food Science and Nutrition, Hallym University, 39 Hallymdaehak-gil, Chuncheon 200-702, Korea.

Received 4 December 2009; Revised 15 March 2010; Accepted 25 March 2010

DOI 10.1002/mc.20640

Published online 6 May 2010 in Wiley InterScience (www.interscience.wiley.com)

spread to other locations in the body [reviewed in [6]]. Therefore, the suppression of inflammation and the normalization of aberrant production of proinflammatory mediators may prove to be a rational approach to chemoprevention. An increasingly compelling body of evidence exists to support the notion that a variety of antiinflammatory phytochemicals can also exert anticarcinogenic effects [1,7].

Nuclear factor-kappa B (NF-κB), the principal molecule in the inflammatory response [reviewed in [8]], is a transcription factor formed by the dimerization of proteins in the Rel family. In an unstimulated state, NF-κB dimers are localized in the cytoplasm as inactive complexes by associating with members of the inhibitor of κB (IκB) family. Upon activation by a variety of stimuli, IκB kinase (IKK) phosphorylates IκB, thereby resulting in the degradation of the protein, which induces the liberation of NF-κB and its subsequent translocation to the nucleus. Within the nucleus, NF-κB binds to the promoter regions of target genes and induces their transcription [reviewed in [9]]. NF-κB regulates the transcriptional activation of genes that encode for inflammatory regulators including cytokines, chemokines, and inducible enzymes such as cyclooxygenase (COX)-2 and inducible nitric oxide synthase (iNOS) [5,10]. NF-κB has been shown to act as a tumor promoter in inflammation-associated cancer [11] and aberrant NF-κB activation is frequently detected in a variety of tumor types [12,13]. Thus, bioactive components with the ability to inhibit aberrant NF-κB activation may be used as cancer preventive agents.

3,3′-Diindolylmethane (DIM, Figure 1) is a major in vivo acid-catalyzed condensation product of indole-3-carbinol, which is an autolysis product of glucobrassicin present in cruciferous vegetables [14]. Several in vivo and in vitro studies have demonstrated that DIM evidences promising anticancer effects [reviewed in [15]]. Recently, we noted that DIM suppresses lipopolysaccharide (LPS)-stimulated inflammatory responses in murine macrophages [16], attenuates dextran sodium sulfate (DSS)-induced colitis, and azoxymethane (AOM)/DSS-induced colon tumorigenesis in mice [17].

In this study, we attempted to determine whether DIM inhibits 12-*O*-tetradecanoylphorbol-13-acetate (TPA)-induced inflammatory responses in mouse skin and explored the possible molecular mechanisms underlying these effects. We demonstrated that DIM potently suppressed TPA-induced inflammation, which may be mediated via the down-regulation of inflammatory mediators. We also demonstrated that DIM suppressed 7,12-dimethylbenz[α]anthracene (DMBA)-initiated and TPA-promoted skin papilloma formation in mice.

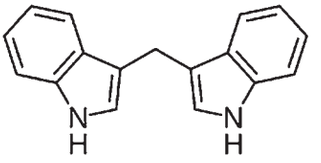

Figure 1. The structure of 3,3′-diindolylmethane (DIM).

MATERIALS AND METHODS

Materials

The reagents used herein were purchased from the indicated suppliers: DIM (Figure 1) from LKT Laboratories (St. Paul. MN); TPA, DMBA, and anti-β-actin antibody from Sigma–Aldrich Co. (St. Louis, MO); antibodies against iNOS and COX-2 from BD Biosciences Pharmingen (Franklin Lakes, NJ); anti-NFκB p65 antibody and GST-IκBα from Santa Cruz Biotechnology (Santa Cruz, CA); antibodies against of P-NFκB p65 (Ser536), IκBα, P-IκBα (Ser32), IKKα, IKKβ, P-IKKα (Ser180)/IKKβ (Ser181), extracellular signal-regulated kinases (ERK)-1/2, P-ERK-1/2, Akt, P-Akt, p38 mitogen-activated protein kinase (MAPK), and P-p38 MAPK from Cell Signaling Technology, Inc. (Beverly, MA); if not noted otherwise, all other materials were obtained from Sigma Co. (St. Louis, MO).

Animals

Female ICR mice (5 wk of age) were purchased from Koatech (Pyeongtaek, Korea). The mice were housed in the animal research facility of Hallym University with temperature maintained at $24 \pm 2^{\circ}C$, $50 \pm 10\%$ relative humidity, and a 12 h light/dark cycle. Mice were allowed to acclimate for 1 wk prior to use and fed with a nonpurified commercial mouse diet (Superfeed Co., Wonju, Korea) and water ad libitum. All experiments were conducted in accordance with the protocols approved by the Animal Care and Use Committee of the Hallym University, Korea.

TPA-Induced Ear Edema Formation in Mice

TPA (5 nmol) was dissolved in 50 μL of vehicle (acetone/DMSO = 85:15, v/v) and applied topically to each ear of female ICR mice (6 wk of age). DIM (0, 10, 20, or 30 μmol) was dissolved in 50 μL of vehicle and topically applied 30 min prior to TPA treatment. The control ears were treated topically with the same volumes of vehicle alone. Mice were killed via CO_2 asphyxiation 5 h after TPA treatment. A mouse ear punch was obtained with a 5 mm dermal biopsy punch and then weighed. The thickness of the punch was measured using a pair of calipers (Mitutoyo Corporation, Kawasaki, Japan).

TPA-Induced Inflammation in Mouse Skin

The dorsal regions of female ICR mice (6 wk of age) were shaved with an electric clipper. The shaved dorsal skins were then treated topically with the indicated dosage of DIM dissolved in 0.2 mL of

vehicle (acetone/DMSO = 85:15, v/v) 30 min prior to the topical treatment of 10 nmol of TPA in 0.2 mL vehicle. The control mice were treated topically with the same volumes of vehicle alone. The dorsal application region measured approximately 2 cm × 2 cm. Mice were sacrificed by CO_2 asphyxiation 2, 4, or 8 h after TPA treatment. The dorsal skin was excised, and the fat from the whole skin was removed on ice. The fat-free skin tissues were then frozen immediately in liquid nitrogen.

Preparation of Lysates From Mouse Skin

The fat-free skin tissues were pulverized immediately with a mortar and pestle in liquid nitrogen. The pulverized skin was homogenized with a Polytron tissue homogenator in ice-cold lysis buffer (50 mmol/L Tris, pH 7.0, 150 mmol/L NaCl, 2 mmol/L EDTA, 10 g/L Triton X-100, 10 g/L Nonidet P-40, 2.5 g/L deoxycholic acid) containing 1 mmol/L sodium orthovanadate, 1 mmol/L phenylmethylsulfonyl fluoride (PMSF), and a protease inhibitor cocktail tablet (Roche, Mannheim, Germany), then solubilized for 40 min at 4°C. The insoluble material was removed via 10 min of centrifugation at 14 800*g* and the supernatant was collected. The protein content of the supernatant was determined using a BCA protein assay kit (Pierce, Rockford, IL).

Preparation of Nuclear Extracts From Mouse Skin

The pulverized fat-free skin was homogenized in hypotonic buffer [(10 mmol/L 4-(2-hydroxyethyl)-1-piperazineethanesulfonic acid (HEPES), pH 7.9, 2 mmol/L $NaCl_2$, 10 mmol/L KCl, 1 mmol/L dithiothreitol (DTT), and 0.1 mmol/L EDTA)] containing 1 mmol/L of sodium orthovanadate, 1 mmol/L of PMSF, and a protease inhibitor cocktail tablet (Roche). After 15 min of incubation on ice, NP-40 (0.7%) was added to the homogenates and the mixture was centrifuged for 2 min at 14 800*g*. The precipitated nuclei were then washed in hypotonic buffer plus 0.625% NP-40, centrifuged, and resuspended in 50 mmol/L HEPES, pH 7.9, 50 mmol/L KCl, 300 mmol/L NaCl, 0.1 mmol/L EDTA, 1 mmol/L DTT, and 100 mL/L, glycerol, and 0.1 mmol/L PMSF. The mixture was incubated for 1 h on ice, then centrifuged for 5 min at 14 800*g* at 4°C. The supernatant was collected and used as the nuclear extract. The protein contents of the nuclear extracts were determined with a BCA protein assay kit (Pierce).

Western Blot Analysis

Western blot analyses of skin lysates and nuclear extracts were conducted as previously described [18]. Signals were detected via an enhanced chemiluminescence method using Immobilon™ Western Chemiluminescent HRP Substrate (Millipore Corporation, Billerica, MA). We used β-actin and the nuclear protein lamin B, respectively, as loading controls for the Western blot analyses of the total cell lysates and nuclear extracts.

The relative abundance of each band was quantified using Bio-profile Bio-1D software (Vilber-Lourmat, Marine la Vallee, France), and the expression levels were normalized to β-actin or lamin B.

cDNA Microarray

Total RNA was isolated using with TRIzol® reagent (Invitrogen, Carlsbad, CA) in accordance with the manufacturer's instructions. cDNA microarrays were conducted using a mouse whole genomic chip (38.5K) in GenomicTree (Daejeon, Korea) as previously described [16]. The microarrays were conducted via comparison of the gene expression of each treatment group (10 nmol TPA, 30 μmol DIM, or 10 nmol TPA + 30 μmol DIM) with that of the control group. Fold changes in gene expression by TPA, DIM, TPA + DIM relative to the controls are listed.

Reverse Transcription-Polymerase Chain Reaction (RT-PCR)

Total RNA was isolated with TRIzol® reagent (Invitrogen) in accordance with the manufacturer's instructions. cDNA was synthesized using 2 μg of total RNA with SuperScript II reverse transcriptase (Invitrogen), and PCR analyses were conducted as previously described [18]. After a 2-min initial denaturation period at 95°C, 30 amplification cycles were performed for iNOS (denaturation for 1 min at 95°C, annealing for 1 min at 60°C, and extension for 1.5 min at 72°C), COX-2 (denaturation for 1 min at 95°C, annealing for 1 min at 60°C, and extension for 1 min at 72°C), chemokine (C-X-C motif) ligand (CXCL)5 (denaturation for 1 min at 95°C, annealing for 1 min at 60°C, and extension for 1 min at 72°C), interleukin (IL)-6 (denaturation for 30 s at 95°C, annealing for 30 s at 60°C, and extension for 1 min at 72°C), and β-actin (denaturation for 1 min at 95°C, annealing for 1 min at 60°C, and extension for 1 min at 72°C). The following PCR primers were employed in this study: iNOS, forward 5′-AAT GGC AAC ATC AGG TCG GCC ATC ACT-3′ and reverse 5′-GCT GTG TGT CAC AGA AGT CTC GAA CTC-3′; COX-2, forward 5′-GGA GAG ACT ATC AAG ATA GT-3′ and reverse 5′-ATG GTC AGT AGA CTT TTA CA-3′; CXCL5, forward 5′-GAG AGC TGC GTT GCG TTT G-3′ and reverse 5′-TTT CCT TGT TTC CAC CGT CCA-3′; IL-6, forward 5′-GAT GCT ACC AAA CTG GAT ATA ATC-3′ and reverse 5′-GGT CCT TAG CCA CTC CTT CTG TG-3′; β-actin, forward 5′-GTT TGA GAC CTT CAA CAC CCC-3′ and reverse 5′-GTG GCC ATC TCC TGC TCG AAG TC-3′. The PCR products were separated on 1% agarose gel and stained with ethidium bromide. The relative abundance of bands corresponding to each specific PCR product to its own β-actin was quantified using the Bio-profile

Bio-1D application (Vilber-Lourmat), and the expression levels were normalized to β-actin.

Electrophoretic Mobility Shift Assay (EMSA)

The double-stranded NF-κB oligonucleotide probe (5′-AGT TGA GGG GAC TTT CCC AGG C-3′) was labeled with [γ-^{32}P]ATP by T4 kinase and purified on a Nick column (Amersham Pharmacia Biotech, Buckinghamshire, UK). Nuclear extracts (10 μg) were incubated with 30 μL of binding buffer (10 mmol/L Tris–HCl, 100 mmol/L NaCl, 1 mmol/L EDTA, 1 mmol/L DTT, 4% glycerol) and 1 μg poly(dIdC) for 30 min at 37°C. For the competitive and supershift experiments, the nuclear extracts were preincubated with a 20-fold molar excess of unlabeled probes and 1 μg of antibody, respectively, for 15 min. Each sample was subjected to 5% nondenaturing gel, and the gels were dried and visualized via autoradiography. The relative abundance of each band on the autoradiograph was quantified via densitometric scanning of the exposed film using the Bio-profile Bio-1D application (Vilber-Lourmat).

In Vitro Kinase Assay

In vitro kinase assays to characterize the catalytic activities of ERK-1/2 were conducted using nonradioactive kinase assay kits (Cell Signaling Technology, Inc.) in accordance with the manufacturer's instructions.

In vitro kinase assays for IKK activity were conducted as previously described [19]. Tissue lysates (750 μg) were immunoprecipitated with IKK antibody followed by incubation with protein A-Sepharose beads (Amersham Biosciences, Buchinghamshire, UK). The kinase reaction was conducted via the addition of the substrate GST-IκBα to the bead in the presence of 10 μCi [γ-^{32}P]ATP at 30°C for 30 min. The reaction was terminated by adding 2× SDS sample buffer and 5 min of subsequent boiling. Each sample was subjected to 10% SDS–PAGE, and the gels were dried and bands were visualized via autoradiography. The relative abundance of each band on the autoradiograph was quantified by densitometric scanning of the exposed film using the Bio-profile Bio-1D application (Vilber-Lourmat).

Two-Stage Skin Carcinogenesis in Mice

Female ICR mice (6 wk of age) were divided randomly into three groups, each consisting of 20 animals. The dorsal regions of the mice were shaved with an electric clipper. The shaved dorsal skin was then treated topically with a single dose of 0.2 μmol DMBA dissolved in 0.2 mL of vehicle (acetone/DMSO = 85:15, v/v). One week after the application of DMBA, the mice were treated topically with 10 nmol of TPA in 0.2 mL of vehicle twice weekly for 20 wk. To assess the antitumor-promoting activity of DIM, 10 μmol of DIM dissolved in 0.2 mL of vehicle was applied topically 30 min prior to each TPA treatment. Control mice were treated topically with the same volumes of vehicle alone. The incidence and number of tumors that were at least 1 mm in diameter were monitored and counted on a weekly basis. The results were expressed as the percentage of tumor-bearing mice (tumor incidence) and the average number of tumors per mouse (tumor multiplicity).

Statistical Analysis

The results were expressed as the means ± SEM and analyzed via analysis of variance. Differences between the treatment groups were evaluated via Duncan's multiple range test or Student's *t*-test, except that differences in tumor incidence between DMBA/TPA and DMBA/TPA/DIM groups were analyzed via a two-sample test for binomial proportions. All statistical analyses were conducted utilizing the SAS system for Windows version 9.1 (SAS Institute, Cary, NC). Differences were considered significant at $P < 0.05$.

RESULTS

DIM Suppresses TPA-Induced Ear Edema Formation in Mice

In order to assess the antiinflammatory effects of DIM, we utilized a mouse ear edema model. The topical application of 5 nmol of TPA to the ears of the mice resulted in 1.5- and 1.2-fold increases in the weight and thickness of the ear as compared to vehicle treatment only. DIM pretreatment induced a dose-dependent suppression of the TPA-induced increases in ear weight and thickness ($P < 0.004$). Pretreatment with 30 μmol of DIM reduced the weight of the ear by 46.0% as compared to TPA treatment alone. The thickness of the ear was reduced by 41.7% in mice pretreated with 30 μmol of DIM as compared to the TPA-treated mice (Figure 2).

DIM Inhibits TPA-Induced COX-2 and iNOS Expression in Mouse Skin

In an effort to characterize the mechanisms by which DIM suppresses TPA-induced inflammatory responses, we initially assessed the expression of COX-2 and iNOS proteins and mRNAs in mouse skin onto which TPA had been applied. The single topical application of 10 nmol TPA onto the shaved dorsal skin of female ICR mice induced the expression of COX-2 and iNOS proteins, with peak levels reached at 8 h (Figure 3A). Pretreatment of the skin with DIM 30 min prior to the application of TPA significantly suppressed TPA-induced increases in COX-2 ($P < 0.03$) and iNOS ($P < 0.04$) protein levels in a dose-dependent manner. DIM pretreatment (10, 20, and 30 μmol) reduced the TPA-induced expression of the COX-2 protein by 34.4%, 67.2%, and 70.5%,

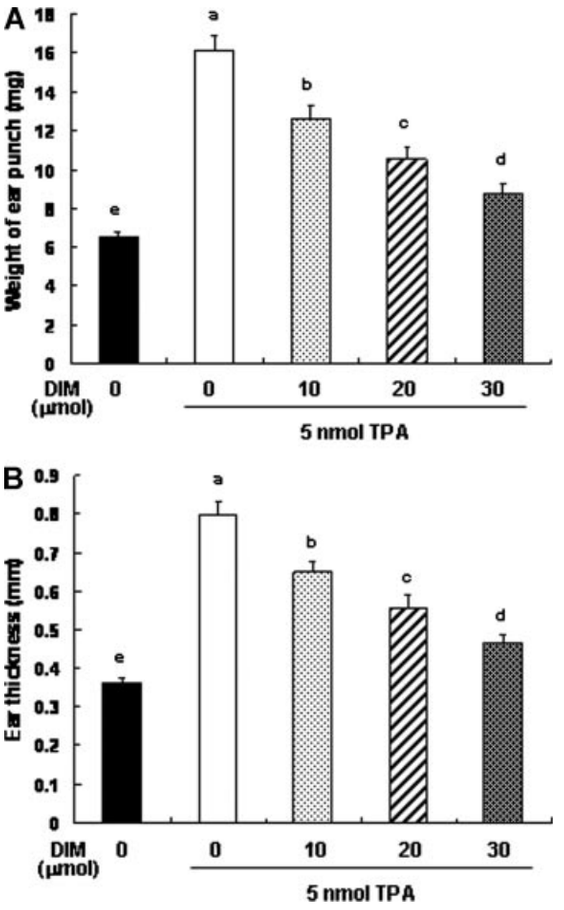

Figure 2. DIM suppresses TPA-induced ear edema formation in mice. TPA (0 or 5 nmol) was topically applied to the ears of female ICR mice. DIM (0, 10, 20, or 30 μmol) was topically applied to the ears of female ICR mice 30 min prior to TPA treatment. Five hours after TPA application, the mice were sacrificed, and ear punches were prepared. (A) Weight of ear punch, (B) Ear thickness, (A, B) Each bar represents the mean ± SEM ($n = 10$). Means without a common letter differ, $P < 0.05$.

respectively. TPA-induced iNOS protein expression levels were reduced by 61.6% in mice pretreated with 30 μmol DIM (Figure 3B). Additionally, DIM induced a dose-dependent suppression of TPA-induced increases in the levels of COX-2 ($P < 0.003$) and iNOS ($P < 0.002$) mRNA expression (Figure 3C).

DIM Inhibits TPA-Induced Expression of CXCL5 and IL-6 mRNAs in Mouse Skin

In order to assess changes in gene expression after TPA and DIM treatment, we conducted cDNA microarrays utilizing a mouse whole genome chip. Among genes associated with inflammation and immune-like responses, those upregulated by TPA and downregulated by DIM are listed in Table 1. The genes coding for CXCL5 and IL-6 were upregulated dramatically by TPA, evidencing 1448.8- and 740.2-fold increases, respectively. DIM pretreatment reduced the TPA-induced mRNA expression of CXCL5 and IL-6 by 26.4- and 3.3-fold, respectively (Table 1). The results of RT-PCR analysis confirmed that TPA increased the steady-state levels of CXCL5 and IL-6 transcripts, and that these increases were significantly reduced by DIM treatment ($P < 0.004$, Figure 4).

DIM Inhibits TPA-Induced NF-κB Activation in Mouse Skin

As NF-κB activation has been recognized as critical for the transcriptional activation of COX-2, iNOS, CXCL5, and IL-6 genes [3–5,20], we subsequently evaluated the effects of DIM on NF-κB activation in TPA-treated mouse skin. The results of EMSA using the oligonucleotide harboring the NF-κB consensus motif showed that the topical application of 5 nmol of TPA markedly increased the NF-κB DNA binding activity by 2.2-fold as compared to vehicle treatment only. DIM significantly inhibited TPA-induced NF-κB DNA binding activity in mouse skin ($P < 0.03$). The results of supershift analysis showed that the TPA-induced band harbored p50/p65 proteins, as this complex was partially supershifted upon the addition of anti-p50 or anti-p65 antibody to the reaction mixture before the addition of the radiolabeled oligonucleotide (Figure 5A). The results of Western blot analysis showed that DIM induced a reduction in the TPA-induced nuclear translocation of the p65 protein ($P < 0.04$, Figure 5B) and inhibited TPA-induced p65 phosphorylation at serine 536 ($P < 0.04$, Figure 5C). Pretreatment with 30 μmol of DIM reduced the TPA-induced nuclear translocation of the p65 protein and p65 phosphorylation by 62.5% and 68.7%, respectively. Additionally, DIM attenuated the TPA-induced phosphorylation and subsequent degradation of IκBα ($P < 0.05$, Figure 5D).

DIM Suppresses the TPA-Induced Activation of IKK and ERK-1/2 in Mouse Skin

Because DIM suppressed the TPA-induced phosphorylation and degradation of IκBα, we subsequently evaluated the effects of DIM on TPA-induced IKK activation. TPA treatment increased IKK-α/β phosphorylation at serine 180/181 by 2.5-fold as compared to vehicle treatment only. DIM (10, 20, and 30 μmol) significantly reduced the TPA-induced phosphorylation of IKK-α/β by 22.9%, 25.7%, and 31.4%, respectively ($P < 0.05$). We also conducted an in vitro kinase assay to assess the catalytic activities of IKK-β. Increased IKK-β activation as the result of TPA treatment was significantly mitigated by DIM treatment ($P < 0.05$, Figure 6A).

MAPKs and Akt have been identified as important regulators of NF-κB activation, and the subsequent expression of inflammatory mediators, including COX-2, in TPA-treated mouse skin [21–23]. The topical application of TPA effectively induced ERK-1/2, p38 MAPK, and Akt phosphorylation in mouse skin. Whereas DIM did not abrogate the TPA-

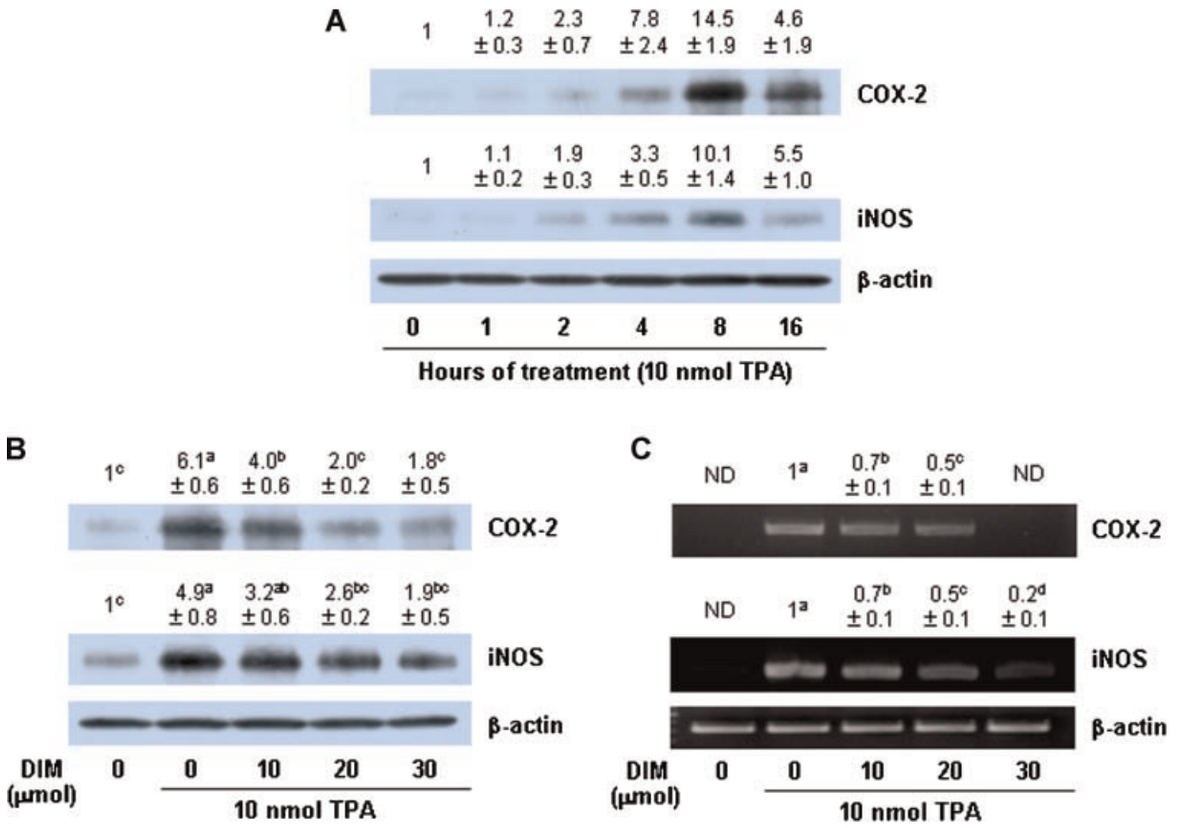

Figure 3. DIM inhibits the TPA-induced expression of COX-2 and iNOS in mouse skin. (A) Dorsal skins of female ICR mice were treated topically with 10 nmol TPA for the indicated time periods. Total tissue lysates were prepared for Western blotting with their relevant antibodies. (B) Dorsal skins of mice were treated topically with DIM (0, 10, 20, or 30 μmol/mouse) 30 min prior to the topical treatment with 10 nmol TPA. Mice were sacrificed at 8 h after TPA treatment. Total tissue lysates were analyzed via Western blotting with the indicated antibodies. (C) Mice were treated as described in Figure 2B, and sacrificed 6 h after TPA treatment. Total RNA was isolated and RT-PCR was performed. Photographs of chemiluminescent detection of the blots (A and B) and ethidium bromide-stained gels (C), which were representative of five independent experiments, are shown. The relative abundance of each band to its own β-actin was quantified and the control levels were set at 1. The adjusted mean ± SEM ($n = 5$) is shown above each blot. Means without a common letter differ, $P < 0.05$.

Table 1. Genes Upregulated by TPA and Downregulated by DIM in Mouse Skin

NCBI accession no.	Fold change (vs. C) TPA	Fold change (vs. C) TPA + DIM	Gene symbol	Description
Inflammation and immune-like responses				
NM_009141	1448.8	26.4	CXCL5	Chemokine (C-X-C motif) ligand 5
NM_009140	1222.0	32.6	CXCL2	Chemokine (C-X-C motif) ligand 2
NM_031168	740.2	3.3	IL-6	Interleukin 6
NM_013652	625.2	13.1	CCL4	Chemokine (C-C motif) ligand 4
NM_013654	348.1	26.7	CCL7	Chemokine (C-C motif) ligand 7
NM_026820	327.7	17.2	IFITM1	Interferon-induced transmembrane protein 1
NM_009892	300.5	10.1	CHI3l3	Chitinase 3-like 3
XM_127883	245.9	14.0	IRG1	Immunoresponsive gene 1
NM_011333	136.4	8.3	CCL2	Chemokine (C-C motif) ligand 2
NM_009883	130.1	8.5	CD14	CD14 antigen
NM_013650	130.0	23.2	S100A8	S100 calcium binding protein A8 (calgranulin A)
NM_009917	122.1	14.7	CCR5	Chemokine (C-C motif) receptor 5
NM_01119	119.0	4.5	PTGS2	Prostaglandin-endoperoxide synthase 2

cDNA microarray were performed using a mouse whole genome chip (38.5K). Among upregulated genes by TPA, genes associated with inflammation and immune-like responses were shown.

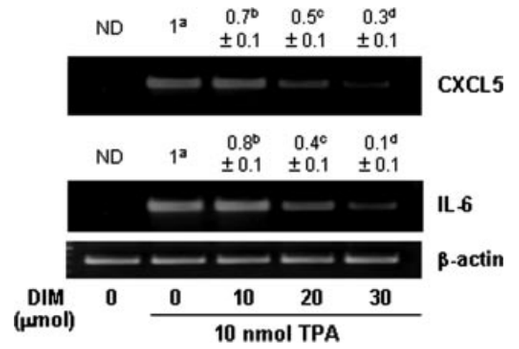

Figure 4. DIM inhibits the TPA-induced mRNA expression of CXCL5 and IL-6 mRNA in mouse skin. Mice were treated as described in Figure 3B, and sacrificed 6 h after TPA treatment. Total RNA was isolated and RT-PCR was performed. Photographs of the ethidium bromide-stained gels, which were representative of five independent experiments, are shown. The relative abundance of each band to its own β-actin was quantified and the control levels were set to 1. The adjusted mean ± SEM ($n = 5$) is shown above each blot. Means without a common letter differ, $P < 0.05$.

induced phosphorylation of p38 MAPK or Akt, the phosphorylation of ERK-1/2 was suppressed significantly by DIM treatment ($P < 0.04$). Additionally, DIM inhibited the TPA-induced catalytic activity of ERK-1/2 ($P < 0.02$). Pretreatment with 30 μmol of DIM suppressed the TPA-induced catalytic activity of ERK-1/2 by 77.8% (Figure 6B).

DIM Suppresses DMBA-Initiated and TPA-Promoted Tumorigenesis in Mouse Skin

Finally, we attempted to ascertain whether DIM suppresses TPA-promoted tumor formation in the skin of DMBA-treated mice. Because the topical application of DIM (10–30 μmol) dose-dependently inhibited TPA-induced ear edema formation (Figure 2) and TPA-induced COX-2 and iNOS expression (Figure 3) as well as other inflammation-related changes (Figures 4–6), we selected the lowest dose of DIM (10 μmol) to evaluate the effects of repeated applications of DIM on skin papilloma formation in mice. In a preliminary experiment, we noted that the repeated topical application of 10 μmol of DIM twice per week caused no visible adverse skin changes. The onset of papillomas could be observed in DMBA-treated mouse skin 6 wk after TPA application. Without DIM treatment, the incidence of papillomas was 100% with 20.4 ± 1.8 papillomas/mouse at the end of the experiment (20th week) (Figure 7). Repeated pretreatment with 10 μmol of DIM prior to the topical applications of TPA resulted in a 20% reduction in papilloma incidence ($P < 0.017$) at the 20th week (Figure 7A). Additionally, DIM pretreatment reduced the multiplicity of papillomas to 8.8 ± 2.1 papillomas/mouse at the 20th week (Figure 7B). No papillomas were detected in the vehicle-treated control mice (data not shown).

To verify that the chemopreventive effect of DIM on TPA-promoted tumor formation in DMBA-initiated mice is mediated by the inhibition of inflammation and inflammatory mediator expression, we evaluated the effects of DIM on COX-2 and iNOS expression, ERK phosphorylation, and NF-κB translocation in DMBA-initiated and TPA-promoted mouse skin containing papillomas. The expressions of COX-2 and iNOS were increased by 2.4- and 1.9-fold, respectively, in the skin of the DMBA/TPA-treated mice as compared to those in the vehicle-treated mice. The levels of the COX-2 and iNOS proteins were significantly lower in the DIM-pretreated skin; the levels of COX-2 and iNOS in the DIM group were 61.8% and 62.1% lower than those of the DMBA/TPA-treated group, respectively ($P < 0.05$). Additionally, ERK-1/2 phosphorylation was increased by 360% in the DMBA/TPA group, which was reduced by 60.9% in the DIM-treated group (Figure 7C). Furthermore, the levels of nuclear p65 were increased by 120% in the DMBA/TPA-treated mice, and 10 μmol of DIM pretreatment reduced this increase significantly ($P < 0.03$, Figure 7D).

DISCUSSION

Several previous studies have reported that DIM inhibits tumor growth in animal cancer models [reviewed in [15]]. However, only a small number of relatively limited studies have addressed the cancer chemopreventive effects of DIM in animal models. Owing to the casual relationship between chronic inflammation and cancer [6,8], the suppression of inflammation has been recognized as a rational approach to chemoprevention. We have shown previously that DIM inhibits LPS-induced iNOS expression as well as the PGE_2 and NO production in murine macrophages [16] and AOM and DSS-induced colon tumorigenesis in mice [17]. In this study, we noted that the topical application of DIM prior to TPA treatment resulted in a marked inhibition of TPA-induced inflammation in mouse skin (Figure 2). We have also demonstrated that DIM effectively suppressed DMBA-initiated and TPA-promoted tumor formation in mouse skin (Figure 7). These results indicate that DIM might prove useful as an antiinflammatory and/or cancer chemopreventive agent. It remains to be determined whether DIM inhibits inflammation and/or cancer development in human skin.

COX-2 and iNOS are inducible enzymes involved in mediating inflammatory responses. Increasing evidence indicates that aberrant regulation of COX-2 and/or iNOS may be closely implicated in the etiology of a variety of cancers [24–26]. Numerous studies suggest that the inhibition of COX-2 and iNOS upregulation is critical not only for attenuation of inflammation but also for the prevention of cancer [21,27–29]. In this study, we elucidated the

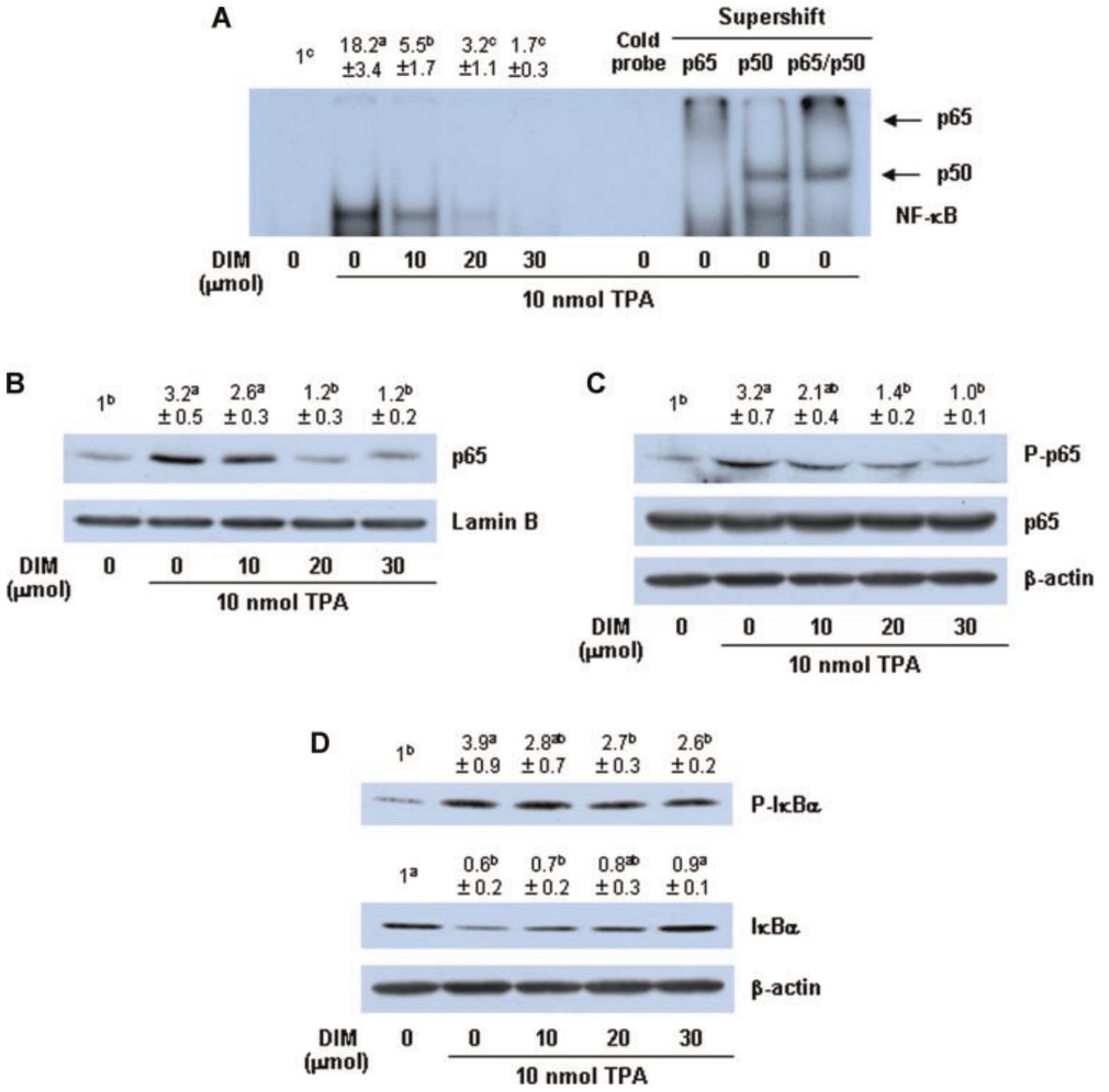

Figure 5. DIM inhibits TPA-induced NF-κB activation in mouse skin. Mice were treated as described in Figure 3B, then sacrificed 4 h after TPA treatment. (A) The epidermal nuclear extracts were prepared and incubated with the phosphorylated NF-κB consensus radiolabeled oligonucleotides for 30 min. Each sample was subjected to 5% nondenaturing gel, and the gels were dried and visualized via autoradiography. An autoradiograph of the dried gel, which was representative of three independent experiments, is shown. The relative abundance of each band was estimated via the densitometric scanning of exposed films. The control levels were set at 1. The adjusted means ± SEM ($n = 3$) are shown above each blot. Means without a common letter differ, $P < 0.05$. The epidermal nuclear extracts (B) and total tissue lysates (C and D) were analyzed via Western blotting with the indicated antibodies. Photographs of chemiluminescent detection of the blots, which were representative of five independent experiments, are shown. The relative abundance of each band to its own β-actin or lamin B was quantified and the control levels were set to 1. The adjusted means ± SEM ($n = 5$) are provided above each blot. Means without a common letter differ, $P < 0.05$.

significant inhibitory effects of DIM against TPA-induced COX-2 and iNOS expression in mouse skin (Figures 3 and 7C). These results show that the inhibition of TPA-promoted tumor formation and inflammation by DIM may be, at least in part, attributable to the suppression of COX-2 and iNOS expression.

CXC chemokines are typically small, secreted molecules that perform a function in leukocyte trafficking, recruitment, and activation. These chemokines also play roles in tumor growth and metastasis by supporting the proliferation or migration of tumor cells, or angiogenesis in tumor tissues [reviewed in [30,31]]. CXCL5, also referred to as epithelial–neutrophil activating peptide (ENA-78), is one of the CXC chemokines, and also has angiogenic properties [32]. It has been reported previously that CXCL5 is upregulated in patients

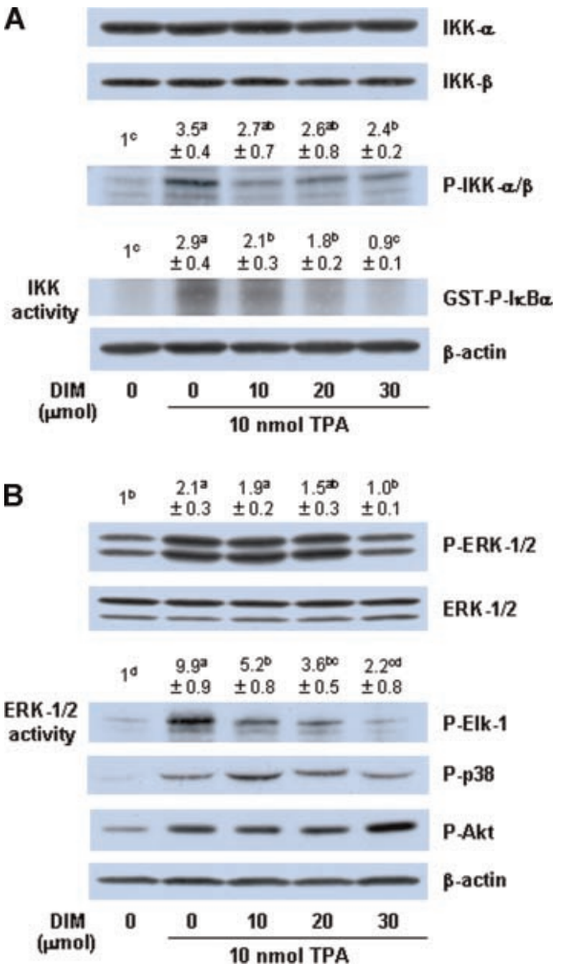

Figure 6. DIM inhibits TPA-induced increases in IKK (A) and ERK (B) activity in mouse skin. Mice were treated as described in Figure 3B, then sacrificed 2 h after TPA treatment. Total tissue lysates were analyzed via Western blotting with the indicated antibodies. Photographs of chemiluminescent detection of the blots, which were representative of five independent experiments, are shown. The relative abundance of each band to their own β-actin was quantified and the control levels were set at 1. The adjusted mean ± SEM ($n = 5$) is shown above each blot. Means without a common letter differ, $P < 0.05$. For in vitro kinase assay, total tissue lysates were immunoprecipitated with primary antibodies specific to IKKβ or ERK, and the kinase reaction was performed. The relative abundance of each band was estimated via densitometric scanning of exposed films. The control levels were set at 1. The adjusted means ± SEM ($n = 3$) are shown above each blot. Means without a common letter differ, $P < 0.05$.

with ovarian [33], renal [34], and pancreatic [35] cancer. In a severe combined immunodeficient mouse model of human nonsmall cell lung cancer (NSCLC), it was demonstrated that COX-2 determines NSCLC tumor growth and that CXCL5 is critical for COX-2-dependent tumor growth [36]. In stomach cancer cells, tumor necrosis factor-α-inducing protein induces CXCL5 gene expression, thus implying that CXCL5 plays a role in the development of stomach cancer [37]. These results indicate that CXCL5 may be very relevant to carcinogenesis, and that the suppression of abnormally upregulated CXCL5 expression might be considered an attractive target for future cancer treatments. To the best of our limited knowledge, this is the first study to assert that TPA dramatically increases the mRNA expression of CXCL5, and this increase was markedly suppressed by DIM treatment in mouse skin. This finding shows that the reduction in CXCL5 expression as a result of DIM treatment is one of the mechanisms by which DIM suppresses inflammation and cancer development in mouse skin.

IL-6 is a typical pleiotropic cytokine which induces the acute phase response, stimulates lymphocytes, and regulates the growth, differentiation, and death of a variety of cell types [reviewed in [38]]. IL-6 has been demonstrated to promote the cancer development and cancer progression [38,39]. We reported previously that DIM reduced LPS-induced IL-6 release by RAW264.7 cells [16] and suppressed the production of IL-6 in colonic tissues obtained from mice exposed to AOM and DSS [17]. In this study, we noted that IL-6 mRNA expression was dramatically increased in TPA-treated mouse skin and was suppressed by DIM treatment (Figure 4). Together, these results show that DIM exerts at least some of its antiinflammatory and anticancer effects via the inhibition of IL-6 expression.

Aberrant regulation of NF-κB activation has been noted in many types of cancer, and NF-κB can affect cancer via the transcriptional activation of genes associated with cell proliferation, suppression of apoptosis, angiogenesis, metastasis, inflammation, and tumor promotion [reviewed in [40]]. In particular, NF-κB may represent a key mechanistic connection between inflammation and cancer [reviewed in [8,41]] and the roles of NF-κB in the induction of COX-2 and iNOS gene transcription have been well established [reviewed in [3–5]]. Many previous studies have demonstrated that a variety of chemopreventive and antiinflammatory phytochemicals downregulate COX-2 and iNOS via the suppression of NF-κB activation [reviewed in [42–44]]. NF-κB has been identified as an essential modulator of CXCL5 [20] and IL-6 transcription [reviewed in [4]]. In this study, we determined that DIM reduced protein and/or mRNA levels of COX-2, iNOS (Figure 3), CXCL5, and IL-6 (Figure 4) in TPA-treated mouse skin. We also demonstrated that DIM suppressed TPA-induced IκB degradation, the nuclear translocation of p65, and NF-κB DNA binding activities (Figure 5). These results indicate that the inhibition of NF-κB signaling contributes to the reduced expression of COX-2, iNOS, CXCL5, and IL-6 in DIM-treated mouse skin.

The transcriptional activation of NF-κB is regulated by upstream kinases, including IKK, ERK, p38 MAKP, and Akt. These kinases lead to the phosphorylation and subsequent proteasomal degradation of NF-κB-bound IκBα, allowing liberated NF-κB dimers

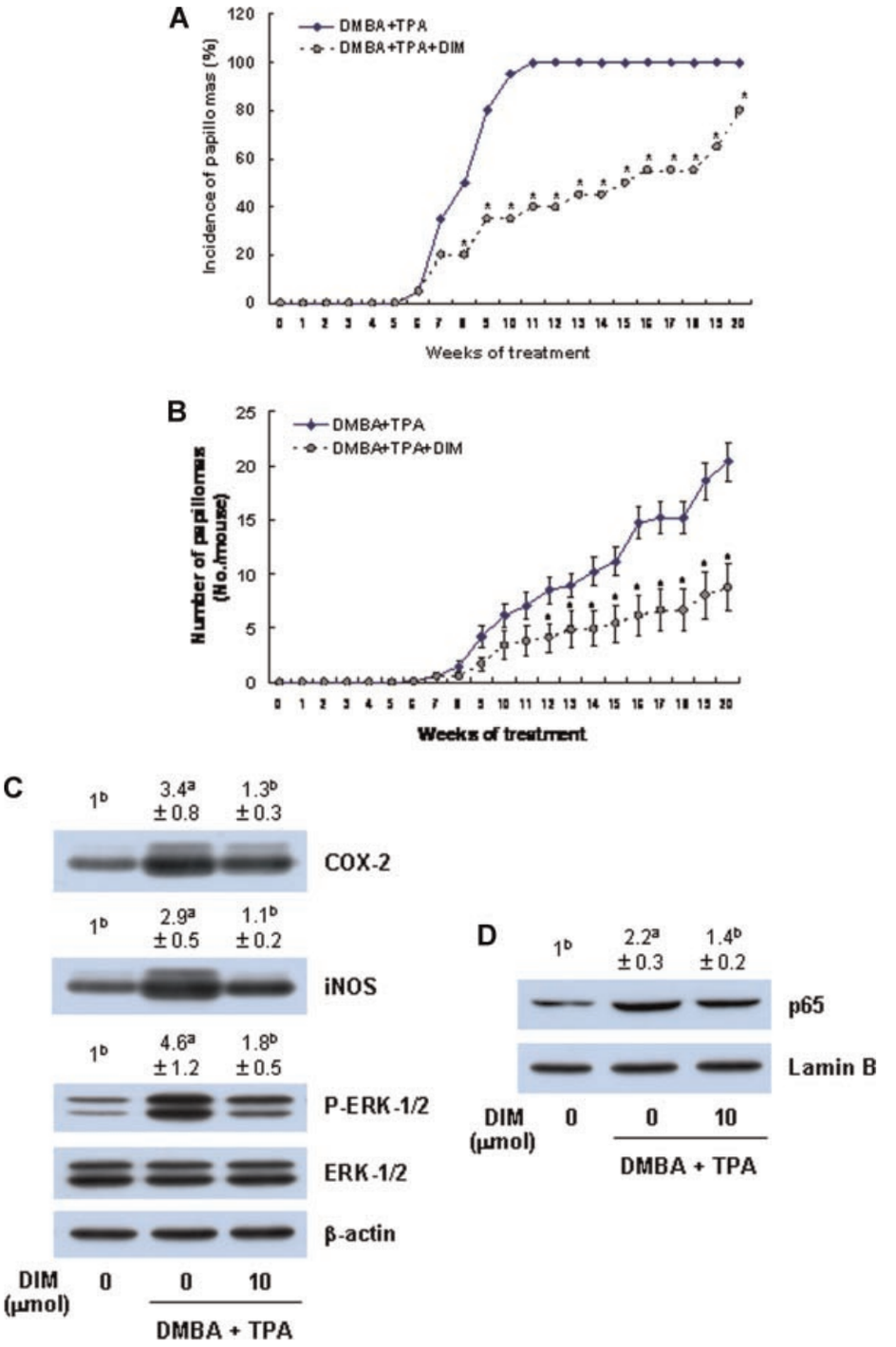

Figure 7. DIM inhibits DMBA-initiated and TPA-promoted two-stage skin carcinogenesis. Mouse skin papillomas were initiated via the topical application of 0.2 μmol of DMBA to the shaved backs of female ICR mice. Beginning after 1 wk, the mice were treated topically with DIM (0 or 10 μmol) 30 min prior to each topical application of 10 nmol TPA twice per week for 20 wk. The incidence and number of papillomas measuring at least 1 mm in diameter were monitored and counted on a weekly basis. The results were expressed as (A) the percentage of tumor-bearing mice (tumor incidence) and (B) the average number of tumors per mouse (tumor multiplicity) ($N = 20$). Statistical differences in tumor incidence and the number of papillomas/mouse between the DMBA/TPA and DMBA/TPA/DIM groups were analyzed via a two-sample test for binomial proportions and Student's *t*-test, respectively. **P*-values of less than 0.05 were considered statistically significant. (C) DIM suppresses the expression of COX-2 and iNOS proteins and the phosphorylation of ERK-1/2 in DMBA-initiated and TPA-promoted mouse skin papillomas. Total tissue lysates were analyzed via Western blotting with the indicated antibodies. Photographs of chemiluminescent detection of the blots, which were representative of five samples from different animals, are shown. The relative abundance of each band to its own β-actin was quantified and the control levels were set at 1. The adjusted mean ± SEM ($n = 5$) is shown above each blot. Means without a common letter differ, $P < 0.05$. (D) DIM suppresses the nuclear translocation of NF-κB in DMBA-initiated and TPA-promoted mouse papillomas. The nuclear extracts of skin samples containing papillomas were analyzed via Western blotting with the indicated antibodies. Photographs of chemiluminescent detection of the blots, which were representative of different samples from five animals, are shown. The relative abundance of each band to its own lamin B was quantified and the control levels were set to 1. The adjusted means ± SEM ($n = 5$) are provided above each blot. Means without a common letter differ, $P < 0.05$.

to translocate to the nucleus [1,44]. Additionally, these molecules regulate NF-κB activity via NF-κB phosphorylation [45,46]. Many previous studies have demonstrated that a variety of phytochemicals that exert chemopreventive and antiinflammatory effects can also inhibit NF-κB activity via the suppression of kinase activity in TPA-stimulated mouse skin [21,22,46]. Because DIM was shown to significantly inhibit NF-κB DNA binding activity (Figure 5A), we attempted to determine whether or not DIM influences the activation of IKK, ERK, p38 MAPK, and Akt. Our results demonstrated that TPA treatment induced the activation of IKK, ERK, p38 MAPK, and Akt. DIM treatment applied prior to TPA application resulted in the reduction of TPA-induced phosphorylation and increases in IKK and ERK activity (Figure 6). These data suggest that DIM suppresses TPA-induced NF-κB activity via the inhibition of IKK and ERK signaling.

In conclusion, the results of this study showed that DIM pretreatment suppresses TPA-induced inflammation and DMBA-initiated and TPA-promoted tumor formation in mouse skin. DIM pretreatment also inhibits COX-2, iNOS, CXCL5, and IL-6 expression, and these effects may be attributable to the inhibition of NF-κB activation. The results of the present study suggest that the inhibition of IKK and ERK activity may contribute to reductions in NF-κB activation in DIM-treated skin. These observations provide some insight into the probable mechanisms underlying the antiinflammatory and antitumor promoting effects of DIM, and therefore suggest that DIM may potentially prove useful as an antiinflammatory agent for skin disease and/or as a chemopreventive agent for skin cancer.

ACKNOWLEDGMENTS

This work was supported by the grant of the Korean Ministry of Education, Science and Technology (The Regional Core Research Program/Medical & Bio-Materials Research Center) and by Basic Science Research Program through the National Research Foundation of Korea (NRF) funded by the Ministry of Education, Science and Technology (314-2008-1-F00069).

REFERENCES

1. Surh YJ. Cancer chemoprevention with dietary phytochemicals. Nat Rev Cancer 2003;3:768–780.
2. Sporn MB, Suh N. Chemoprevention of cancer. Carcinogenesis 2000;21:525–530.
3. Marx J. Cancer research. Inflammation and cancer: The link grows stronger. Science 2004;306:966–968.
4. Li Q, Withoff S, Verma IM. Inflammation-associated cancer: NF-kappaB is the lynchpin. Trends Immunol 2005;26:318–325.
5. Hofseth LJ, Ying L. Identifying and defusing weapons of mass inflammation in carcinogenesis. Biochim Biophys Acta 2006;1765:74–84.
6. Coussens LM, Werb Z. Inflammation and cancer. Nature 2002;420:860–867.
7. Chen C, Kong AN. Dietary cancer-chemopreventive compounds: From signaling and gene expression to pharmacological effects. Trends Pharmacol Sci 2005;26:318–326.
8. Balkwill F, Coussens LM. Cancer: An inflammatory link. Nature 2004;431:405–406.
9. Yamamoto Y, Gaynor RB. IkappaB kinases: Key regulators of the NF-kappaB pathway. Trends Biochem Sci 2004;29:72–79.
10. Giuliani C, Napolitano G, Bucci I, Montani V, Monaco F. NF-kB transcription factor: Role in the pathogenesis of inflammatory, autoimmune, and neoplastic diseases and therapy implications. Clin Ter 2001;152:249–253.
11. Pikarsky E, Porat RM, Stein I, et al. NF-kappaB functions as a tumour promoter in inflammation-associated cancer. Nature 2004;431:461–466.
12. Mayo MW, Baldwin AS. The transcription factor NF-kappaB: Control of oncogenesis and cancer therapy resistance. Biochim Biophys Acta 2000;1470:M55–M62.
13. Lin A, Karin M. NF-kappaB in cancer: A marked target. Semin Cancer Biol 2003;13:107–114.
14. De Kruif CA, Marsman JW, Venekamp JC, et al. Structure elucidation of acid reaction products of indole-3-carbinol: Detection in vivo and enzyme induction in vitro. Chem Biol Interact 1991;80:303–315.
15. Sarkar FH, Li Y. Harnessing the fruits of nature for the development of multi-targeted cancer therapeutics. Cancer Treat Rev 2009;35:597–607.
16. Cho HJ, Seon MR, Lee YM, et al. 3,3′-Diindolylmethane suppresses the inflammatory response to lipopolysaccharide in murine macrophages. J Nutr 2008;138:17–23.
17. Kim YH, Kwon HS, Kim DH, et al. 3,3′-Diindolylmethane attenuates colonic inflammation and tumorigenesis in mice. Inflamm Bowel Dis 2009;15:1164–1173.
18. Cho HJ, Kim WK, Kim EJ, et al. Conjugated linoleic acid inhibits cell proliferation and ErbB3 signaling in HT-29 human colon cell line. Am J Physiol Gastrointest Liver Physiol 2003;284:G996–G1005.
19. Bharti AC, Donato N, Singh S, Aggarwal BB. Curcumin (diferuloylmethane) down-regulates the constitutive activation of nuclear factor-kappa B and IkappaBalpha kinase in human multiple myeloma cells, leading to suppression of proliferation and induction of apoptosis. Blood 2003;101:1053–1062.
20. Richmond A. NF-kappa B, chemokine gene transcription and tumour growth. Nat Rev Immunol 2002;2:664–674.
21. Chung WY, Park JH, Kim MJ, et al. Xanthorrhizol inhibits 12-O-tetradecanoylphorbol-13-acetate-induced acute inflammation and two-stage mouse skin carcinogenesis by blocking the expression of ornithine decarboxylase, cyclooxygenase-2 and inducible nitric oxide synthase through mitogen-activated protein kinases and/or the nuclear factor-kappa B. Carcinogenesis 2007;28:1224–1231.
22. Kundu JK, Hwang DM, Lee JC, et al. Inhibitory effects of oligonol on phorbol ester-induced tumor promotion and COX-2 expression in mouse skin: NF-kappaB and C/EBP as potential targets. Cancer Lett 2009;273:86–97.
23. Medeiros R, Otuki MF, Avellar MC, Calixto JB. Mechanisms underlying the inhibitory actions of the pentacyclic triterpene alpha-amyrin in the mouse skin inflammation induced by phorbol ester 12-O-tetradecanoylphorbol-13-acetate. Eur J Pharmacol 2007;559:227–235.
24. Franco L, Doria D, Bertazzoni E, Benini A, Bassi C. Increased expression of inducible nitric oxide synthase and cyclooxygenase-2 in pancreatic cancer. Prostaglandins Other Lipid Mediat 2004;73:51–58.
25. Rahman MA, Dhar DK, Yamaguchi E, et al. Coexpression of inducible nitric oxide synthase and COX-2 in hepatocellular carcinoma and surrounding liver: Possible involvement of COX-2 in the angiogenesis of hepatitis C virus-positive cases. Clin Cancer Res 2001;7:1325–1332.

26. Wilson KT, Fu S, Ramanujam KS, Meltzer SJ. Increased expression of inducible nitric oxide synthase and cyclooxygenase-2 in Barrett's esophagus and associated adenocarcinomas. Cancer Res 1998;58:2929–2934.
27. Seo HJ, Park KK, Han SS, et al. Inhibitory effects of the standardized extract (DA-9601) of Artemisia asiatica Nakai on phorbol ester-induced ornithine decarboxylase activity, papilloma formation, cyclooxygenase-2 expression, inducible nitric oxide synthase expression and nuclear transcription factor kappa B activation in mouse skin. Int J Cancer 2002; 100:456–462.
28. Lai CS, Li S, Chai CY, et al. Anti-inflammatory and antitumor promotional effects of a novel urinary metabolite, 3′,4′-didemethylnobiletin, derived from nobiletin. Carcinogenesis 2008;29:2415–2424.
29. Lai CS, Li S, Chai CY, et al. Inhibitory effect of citrus 5-hydroxy-3,6,7,8,3′,4′-hexamethoxyflavone on 12-O-tetradecanoylphorbol 13-acetate-induced skin inflammation and tumor promotion in mice. Carcinogenesis 2007;28:2581–2588.
30. Wang JM, Deng X, Gong W, Su S. Chemokines and their role in tumor growth and metastasis. J Immunol Methods 1998;220:1–17.
31. Balkwill F. Cancer and the chemokine network. Nat Rev Cancer 2004;4:540–550.
32. Arenberg DA, Keane MP, DiGiovine B, et al. Epithelial-neutrophil activating peptide (ENA-78) is an important angiogenic factor in non-small cell lung cancer. J Clin Invest 1998;102:465–472.
33. Furuya M, Suyama T, Usui H, et al. Up-regulation of CXC chemokines and their receptors: Implications for proinflammatory microenvironments of ovarian carcinomas and endometriosis. Hum Pathol 2007;38:1676–1687.
34. Hlavkova D, Kopecky O, Lukesova S, et al. Monitoring of serum levels of angiogenin, ENA-78 and GRO chemokines in patients with renal cell carcinoma (RCC) in the course of the treatment. Acta Med (Hradec Kralove) 2008;51:185–190.
35. Frick VO, Rubie C, Wagner M, et al. Enhanced ENA-78 and IL-8 expression in patients with malignant pancreatic diseases. Pancreatology 2008;8:488–497.
36. Pold M, Zhu LX, Sharma S, et al. Cyclooxygenase-2-dependent expression of angiogenic CXC chemokines ENA-78/CXC Ligand (CXCL) 5 and interleukin-8/CXCL8 in human non-small cell lung cancer. Cancer Res 2004;64:1853–1860.
37. Kuzuhara T, Suganuma M, Kurusu M, Fujiki H. *Helicobacter pylori*-secreting protein Tipalpha is a potent inducer of chemokine gene expressions in stomach cancer cells. J Cancer Res Clin Oncol 2007;133:287–296.
38. Kamimura D, Ishihara K, Hirano T. IL-6 signal transduction and its physiological roles: The signal orchestration model. Rev Physiol Biochem Pharmacol 2003;149:1–38.
39. Kovalchuk AL, Kim JS, Park SS, et al. IL-6 transgenic mouse model for extraosseous plasmacytoma. Proc Natl Acad Sci USA 2002;99:1509–1514.
40. Baud V, Karin M. Is NF-kappaB a good target for cancer therapy? Hopes and pitfalls. Nat Rev Drug Discov 2009;8: 33–40.
41. Karin M. Nuclear factor-kappaB in cancer development and progression. Nature 2006;441:431–436.
42. Surh YJ, Chun KS, Cha HH, et al. Molecular mechanisms underlying chemopreventive activities of anti-inflammatory phytochemicals: Down-regulation of COX-2 and iNOS through suppression of NF-kappa B activation. Mutat Res 2001;480–481:243–268.
43. Surh YJ, Na HK. NF-kappaB and Nrf2 as prime molecular targets for chemoprevention and cytoprotection with anti-inflammatory and antioxidant phytochemicals. Genes Nutr 2008;2:313–317.
44. Kundu JK, Surh YJ. Breaking the relay in deregulated cellular signal transduction as a rationale for chemoprevention with anti-inflammatory phytochemicals. Mutat Res 2005;591: 123–146.
45. Yang F, Tang E, Guan K, Wang CY. IKK beta plays an essential role in the phosphorylation of RelA/p65 on serine 536 induced by lipopolysaccharide. J Immunol 2003;170:5630–5635.
46. Chun KS, Keum YS, Han SS, Song YS, Kim SH, Surh YJ. Curcumin inhibits phorbol ester-induced expression of cyclooxygenase-2 in mouse skin through suppression of extracellular signal-regulated kinase activity and NF-kappaB activation. Carcinogenesis 2003;24:1515–1524.